

ISSN: (Print) (Online) Journal homepage: <https://www.tandfonline.com/loi/tbsd20>

Discovery of a new ATP-citrate lyase (ACLY) inhibitor identified by a pharmacophore-based virtual screening study

Vibhu Jha, Salvatore Galati, Valerio Volpi, Lidia Ciccone, Filippo Minutolo, Flavio Rizzolio, Carlotta Granchi, Giulio Poli & Tiziano Tuccinardi

To cite this article: Vibhu Jha, Salvatore Galati, Valerio Volpi, Lidia Ciccone, Filippo Minutolo, Flavio Rizzolio, Carlotta Granchi, Giulio Poli & Tiziano Tuccinardi (2021) Discovery of a new ATP-citrate lyase (ACLY) inhibitor identified by a pharmacophore-based virtual screening study, Journal of Biomolecular Structure and Dynamics, 39:11, 3996-4004, DOI: [10.1080/07391102.2020.1773314](https://doi.org/10.1080/07391102.2020.1773314)

To link to this article: <https://doi.org/10.1080/07391102.2020.1773314>



Published online: 02 Jun 2020.



Submit your article to this journal [↗](#)



Article views: 526



View related articles [↗](#)



View Crossmark data [↗](#)



Citing articles: 1 View citing articles [↗](#)



Discovery of a new ATP-citrate lyase (ACLY) inhibitor identified by a pharmacophore-based virtual screening study

Vibhu Jha^a, Salvatore Galati^a, Valerio Volpi^a, Lidia Ciccone^a , Filippo Minutolo^a , Flavio Rizzolio^{b,c} ,
Carlotta Granchi^a , Giulio Poli^a and Tiziano Tuccinardi^a 

^aDepartment of Pharmacy, University of Pisa, Pisa, Italy; ^bPathology Unit, Centro di Riferimento Oncologico di Aviano (CRO) IRCCS, Aviano, Italy; ^cDepartment of Molecular science and Nanosystems, University Ca' Foscari of Venice, Venice, Italy

Communicated by Ramaswamy H. Sarma

ABSTRACT

ATP citrate lyase (ACLY) is an important enzyme that catalyzes the conversion of citrate to acetyl-CoA in normal cells, facilitating the *de novo* fatty acid synthesis. Lipids and fatty acids were found to be accumulated in different types of tumors, such as brain, breast, rectal and ovarian cancer, representing a great source of energy for cancer cell growth and metabolism. Since ACLY-mediated conversion of citrate to acetyl-CoA constitutes the basis for fatty acid synthesis, ACLY seems to be quite an unexplored and promising therapeutic target for anticancer drug design. A pharmacophore-based virtual screening (VS) protocol with the aid of hierarchical docking, consensus docking (CD), molecular dynamics (MD) simulations and ligand-protein binding free energy calculations led to the identification of compound VS1, which showed a moderate but promising inhibitory activity, demonstrating to be 2.5 times more potent than reference inhibitor 2-hydroxycitrate. These results validate the reliability of our VS workflow and pave the way for the design of novel and more potent ACLY inhibitors.

ARTICLE HISTORY

Received 18 March 2020
Accepted 18 May 2020

KEYWORDS

ACLY; virtual screening;
pharmacophore; consensus
docking; molecular dynamics

Introduction

ATP citrate lyase (ACLY) is a key enzyme of lipogenesis in cells. ACLY acts as a physiological shunt between glucose metabolism and fatty acid synthesis by producing acetyl-CoA (Zaidi et al., 2012). ACLY affects both lipid and cholesterol synthesis and, due to its physiological role in lipogenesis, has long been considered as an important pharmacological target for the treatment of hyperlipidemia and hypercholesterolemia. A significant number of compounds were specifically designed to inhibit ACLY in order to treat these pathological conditions. Reported ACLY inhibitors showed positive results in human clinical trials as cholesterol-lowering drugs (Granchi, 2018). Despite the involvement of ACLY in lipid-associated disorders, recent studies highlighted ACLY as an important therapeutic target in cancer treatment due to its pivotal role in cancer cell metabolism by triggering fatty acid synthesis. In fact, lipid accumulation has been observed in many types of tumors, including brain, breast, ovarian and colorectal cancers, and has recently drawn increased attention. This has motivated scientists to understand the molecular mechanisms by which fatty acids metabolism participates in the pathophysiological processes of cancer (Kuo & Ann, 2018; Zhao et al., 2016). Generally, *de novo* fatty acid synthesis is suppressed in most normal cells, whereas in cancer cells it is highly upregulated. Energy requirement in cancer cells tends to increase due to high cell proliferation rate. To meet the high demands of energy requirement for proliferation, cancer cells undergo major modifications in their

metabolic pathways and metabolic adaptation can be considered as an important attribute in cancer progression. One of the most important metabolic hallmarks of cancer cells is increased *de novo* lipid synthesis, which may include the fatty acid synthesis pathway and mevalonate pathway, the latter leading to the synthesis of cholesterol and isoprenoids (Menendez & Lupu, 2007; Swinnen et al., 2006). Fatty acid synthesis starts with an ACLY-mediated conversion of citrate to acetyl-CoA, which is then metabolized to malonyl-CoA. Fatty acids and metabolic intermediates are used by rapidly proliferating cells in energy production for various biochemical and cellular processes like mitochondrial β -oxidation of fatty acids, palmitoylation of oncogenes and incorporation into complex lipids for maintenance of the membrane integrity (Suburu & Chen, 2012; Zadra et al., 2013). Fatty acid synthesis is associated with both cancer cell growth and transformation; in particular, activated ACLY signaling is associated with many human cancer types including prostate cancer, lung adenocarcinoma, leukemia, glioblastomas, ovarian cancer and liver cancer (Beckner et al., 2010; Bertilsson et al., 2012; Migita et al., 2008; Wang et al., 2012, 2019; Yahagi et al., 2005).

The major involvement of ACLY in cancer (Hatzivassiliou et al., 2005) and the availability of X-ray structures of ACLY in complex with the endogenous ligands (Granchi, 2019; Verschueren et al., 2019) encouraged medicinal chemists to employ receptor-based drug design techniques for the identification of new ACLY inhibitors. Initially, ACLY inhibitors

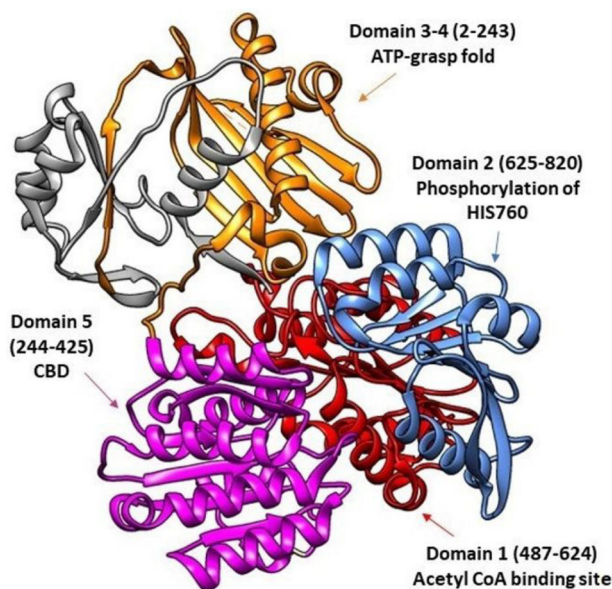


Figure 1. Structure of the human ACLY.

derived from natural sources, for example the 14-membered macrocycle radicicol isolated from the fungus *Monosporium bonorden*. Radicicol proved to inhibit ACLY in a non-competitive manner, with a potency in the low micromolar range (Ki et al., 2000). However, radicicol is not selective for ACLY, because it was shown to potently inhibit Heat shock protein-90 function. Another fungus-derived macrolide is dehydrocurvularin, which was recently identified as a highly potent irreversible inhibitor of ACLY (Deng et al., 2019). ACLY inhibitors of synthetic origin can be exemplified by the sulfonamide derivative BMS-303141, which was synthesized and tested in 2007 (Li et al., 2007), demonstrating a potent in vitro activity. Some years later, compound NDI-091143, belonging to the same chemical class of BMS-303141, was identified as the first ACLY allosteric inhibitor, providing new insights into the catalytic mechanism of the enzyme (Wei et al., 2019). Finally, the lactone derivative SB204990 is a potent and specific inhibitor, which was designed as a pro-drug. It was found to be able to penetrate in cells to regulate plasma lipid levels (Pearce et al., 1998) and to reduce cancer cell growth (Hatzivassiliou et al., 2005).

Receptor-based virtual screening (VS) is nowadays fundamental for the cost-effective development of therapeutic agents, employing the knowledge of the biological target's structure and ligand-protein interactions at the atomic level (Tuccinardi, 2009). Receptor-based pharmacophore models representing key ligand-protein interactions identified in X-ray complexes can be built and used to filter compounds from commercial and in-house databases for the identification of potential hit compounds forming similar interactions with the target protein (Amaravadhi et al., 2014). The compounds selected through receptor-based pharmacophore models are usually subjected to molecular docking, in order to predict their most energetically favored binding mode into the target protein, thus filtering the compound library based on the desirable ligand-protein interactions formed by the compounds, an approach that have been already used in successful VS studies (Lapillo et al., 2019; Russo Spina et al.,

2019; Tuccinardi et al., 2016). A particularly reliable docking approach is constituted by consensus docking (CD), which relies on the search for common binding modes from the top-ranked docked poses produced by multiple different programs, which are employed in combination to one another. The CD approach was found to predict ligand binding poses better than single docking evaluations (Poli et al., 2016; Tuccinardi et al., 2014). Moreover, the combination of pharmacophore screening with CD showed to be a profitable approach for the identification of novel enzyme inhibitors. Based on these considerations, we have developed a pharmacophore-based VS protocol, supported by hierarchical docking, CD and MD simulations in order to identify new ACLY inhibitors. The application of the protocol allowed the discovery of a novel compound endowed with micromolar inhibitory activity against ACLY, thus confirming the reliability of the VS workflow. Ligand-protein binding free energy calculations by Molecular Mechanics-Generalized Born Surface Area (MM-GBSA) methods were then employed in the present study to analyze the predicted binding mode of hit compound VS1 at a deeper level along with exploring key amino acid residues of ACLY binding site.

Results and discussion

The first step of any receptor-based VS study is usually the search and retrieval of X-ray structures of the protein of our interest. The recently deposited X-ray structure of ACLY in complex with the potent allosteric inhibitor NDI-091143 undoubtedly represents a great tool for developing receptor-based strategies aimed at identifying novel ACLY ligands, by exploring the newly discovered enzyme allosteric site. However, at the time we designed and performed our VS study, the co-crystal structure of ACLY bound to NDI-091143 was not available yet, nor information about the allosteric mechanism of action of the inhibitor was known. Therefore, no hints about the allosteric site of NDI-091143 in ACLY and its localization within the protein structure were available to be employed in a receptor-based VS study. For this reason, we selected the crystallographic complex of ACLY with a bound endogenous citrate molecule (PDB ID: 5TDE) as a valuable reference structure for developing our VS protocol aimed at identifying novel ACLY inhibitors. The crystal structure of ACLY includes 5 different binding domains, each playing an important role in catalysis. The site where ATP molecule binds is called the "ATP-grasp fold" and consists of domain 3 and domain 4, which grab ATP between them, whereas citrate finds a place in domain 5, which is called the "citrate binding domain" (CBD), but it is not as deep as the ATP-grasp fold. In the catalytic process, phosphorylation of H760 occurs in domain 2, followed by H-bonding of phosphate with pro-S carboxylate of citrate from domain 5 (as citrate presents three carboxylic groups, in order to distinguish two terminal groups, we denoted them as pro-R and pro-S), which results in the formation of citryl phosphate. The last step of catalysis is facilitated by domain 1, also called as the "acetyl CoA binding site", where CoA attacks citryl phosphate to form citryl-CoA, which is further cleaved to produce

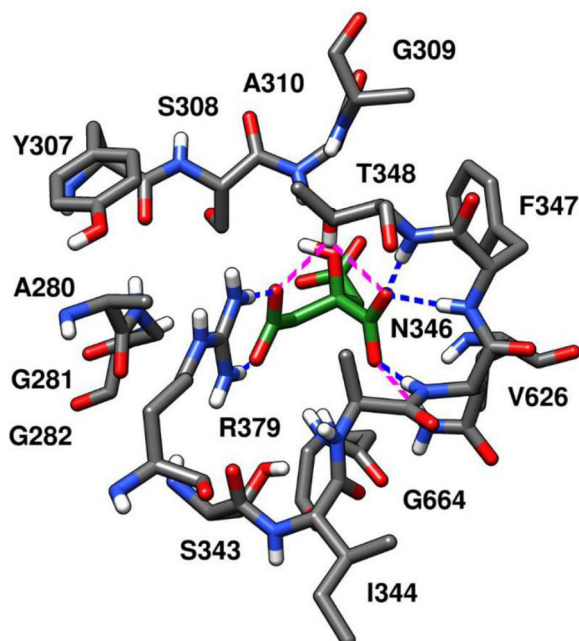


Figure 2. Citrate in the ACLY binding site (PDB ID: 5TDE). The mandatory pharmacophore features refer to the H-bonds colored in blue, whereas the optional features correspond to H-bonds colored in pink.

acetyl-CoA and oxaloacetate. In principle, both the ATP-grasp fold and the CBD could be targeted by our VS protocol. However, we envisioned that focusing on the identification of ATP-competitive inhibitors was not a profitable strategy, due to the high probability of off-target activity against those kinds of enzymes requiring ATP as a co-factor, such as protein kinases. In fact, for the same reason, the search for non-ATP-competitive inhibitors such as substrate phosphorylation site inhibitors is taking ground in drug design campaigns focused on kinase targets (Breen & Soellner, 2015). Therefore, our VS study was set up based on exploring the fundamental interactions observed for citrate in the CBD, which were utilized to develop a structure-based pharmacophore model (Figure 1).

The loop formed by amino acids 343–348 of CBD allows the proper orientation of the endogenous ligand, with the pro-*S* carboxylic group free from interactions with the binding pocket. The subsequent intermediates citryl phosphate and citryl-CoA possess a *S* configuration and the reaction catalyzed by ACLY is, therefore, stereospecific. Within CBD, the pro-*R* carboxyl group of citrate forms a salt bridge with R379 and one less stable hydrogen bond with the hydroxyl group of T348. The central carboxylic fragment establishes hydrogen bonds with the backbone nitrogen of N346, F347 and T348, and two less stable H-bonds with the hydroxyl group of T348 and the side-chain of N346 (Figure 2) (Hu et al., 2017; Sun et al., 2011).

These intramolecular interactions were subsequently employed for the development of a pharmacophore model, which was constructed by using Ligand-Scout program (Wolber & Langer, 2005), considering the fundamental interactions established by citrate in the binding site of ACLY (Figure 3). The pharmacophore model consists of 4 H-bond acceptor features, set as mandatory features, so that all

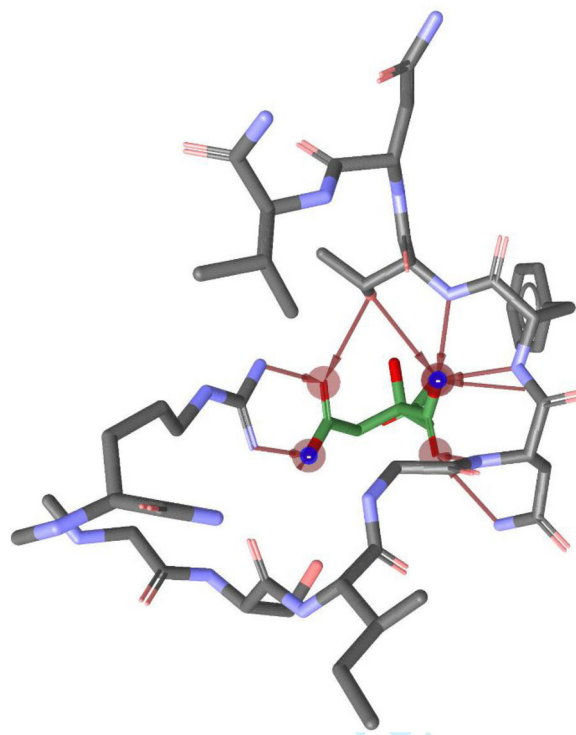


Figure 3. Receptor-based pharmacophore model used for the VS studies.

ligands that do not meet these criteria will be rejected. These mandatory H-bond acceptors represent the interactions with R379 and the backbone of T348, F347 and N346. The pharmacophore model also considers 3 other hydrogen bond acceptors as optional features, i.e. the two H-bond acceptors corresponding to the interactions with the hydroxyl group of T348 and the interaction with the side-chain of N346. Moreover, the model was refined by adding exclusion volume spheres representing the regions of space occupied by the protein residues surrounding citrate, which thus cannot be occupied by ligands during a pharmacophore screening.

The next operational step was the validation of the docking procedure, which involves the assessment of various programs available in our laboratory to identify the methods able to reproduce the binding orientation of the X-ray ligand. Citrate was isolated from the X-ray complex with ACLY (PDB ID: 5TDE) and 12 docking methods were tested by performing a self-docking analysis and calculating the root-mean-square deviation (RMSD) between the position of the endogenous ligand predicted by docking and its known experimental disposition. The results of the self-docking study are summarized in Table 1. Based on the RMSD results, we selected 11 out of 12 docking programs for further study (with the single exclusion of Dock 6), as they were able to reproduce the ligand orientation with a RMSD value lower than 2.0 Å, with respect to the crystallized ligand orientation.

After the development of the pharmacophore model and the selection of the docking programs, we employed a pharmacophoric screening, combined with hierarchical docking and followed by consensus docking (CD), to identify new ACLY inhibitors. The pharmacophore model was applied to screen ligands from Vitas-M and Enamine commercial

Table 1. RMSD results of the self-docking analysis.

Docking method	RMSD (Å)
Dock 6	2.2
Glide SP	1.5
Glide XP	1.7
Gold ASP	1.2
Gold Chemscore	1.7
Gold Goldscore	1.8
Gold PLP	1.8
Autodock	1.9
Plants	1.6
Vina	1.2
Glamdock	1.8
rDock	1.6

databases, corresponding to about 2.5 million compounds. Consequently, a total of 62836 molecules matching at least the four mandatory features and respecting the volume constraints were retained by the pharmacophore model search. Instead of further reducing the number of compounds based on the matching of optional pharmacophore features, we decided to consider all 62836 compounds for docking studies using the selected 11 docking programs; however, these molecules were subjected to a hierarchical docking strategy. The application of a hierarchical approach in our VS workflow allowed to significantly reduce computation time by employing faster docking methods first and then filtering the molecules based on a qualitative post-docking filter, before using slower docking procedures. In this way, the number of analyzed ligands were reduced at each docking step, favoring the application of slower docking methods in our VS study. Starting from the fastest docking procedure, the screened molecules were docked and the top-ranked docked pose from each molecule was then subjected to filter analysis, selecting only molecules able to show the fundamental H-bond interactions corresponding to the mandatory pharmacophoric features (with R379, T348, F347 and N346). Compounds unable to meet this criterion were discarded, while the remaining ligands were docked by the next docking program and checked again for these H-bond interactions. This procedure was repeated for all remaining docking programs. At the end of 11th docking procedure, 3547 compounds were eventually retrieved. The details of filtration of compounds after each docking step is mentioned in Table 2.

Based on these analyses, the resulting 3547 compounds were subjected to CD through an in-house program, clustering the 11 different docking poses obtained for each ligand based on their reciprocal RMSD, with a cutoff of 2.0 Å (see Materials and Methods for details). The total 176 compounds showing a minimum consensus level of 8 were selected and further considered in our VS (Table 3).

Since the binding mode of the selected compounds was assumed to be particularly reliable, being predicted by at least 8 out of the 11 docking methods used, a further filtering analysis was employed to check fundamental and optional H-bond interactions predicted for these ligands: only compounds showing maximum number of H-bond interactions, i.e. meeting all mandatory H-bonds criteria along with optional H-bond interactions, were considered. In total, 25 compounds were selected and subjected to 20 ns MD simulations to verify the stability of their predicted

Table 2. Hierarchical docking procedures and number of filtered compounds.

Step	Docking Procedure	Final no. of Hits
1.	Glide SP	19789
2.	Gold ASP	9721
3.	rDock	8131
4.	Plants	6556
5.	Glide XP	5473
6.	Gold Chemscore	4894
7.	Gold Goldscore	4540
8.	Glamdock	4335
9.	Gold PLP	3874
10.	Autodock	3722
11.	Vina	3547

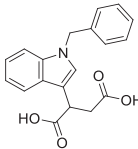
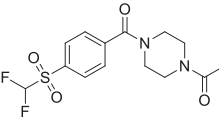
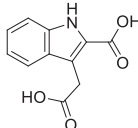
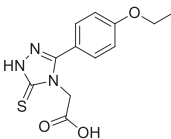
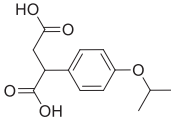
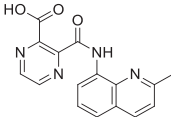
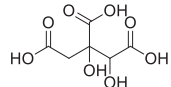
Table 3. Consensus docking results.

Consensus level	No. of compounds
11	2
10	27
9	37
8	110
7	191
6	341
5	598
4	1008
3	1057
2	175
1	1

binding mode. The trajectories of ligand-protein complexes resulting from MD studies were analyzed in terms of H-bond stability and ligand RMSD with respect to the starting coordinates. Out of 25 compounds, 6 ligands were eventually selected, since they showed an average RMSD value lower than 2.0 Å and the maintenance of all 4 mandatory H-bonds for more than 95% of the whole simulation. These compounds were thus tested for their inhibitory properties against ACLY. The known ACLY inhibitor 2-hydroxycitrate (HCA) was used as a reference compound for the assay (Hoffmann et al., 1980). As shown in Table 4, among the 6 tested compounds, VS1 was the only one possessing a relevant inhibitory activity, showing an IC₅₀ value of 191 μM; however, the ligand demonstrated to be about 2.5-fold more active than the reference inhibitor HCA (IC₅₀ = 465 μM) in our assay conditions.

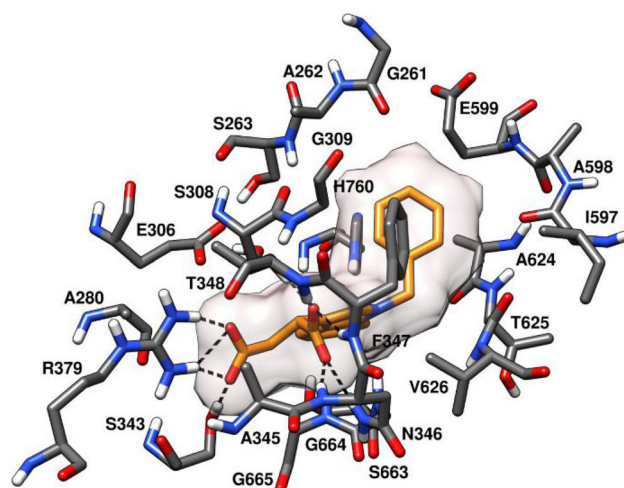
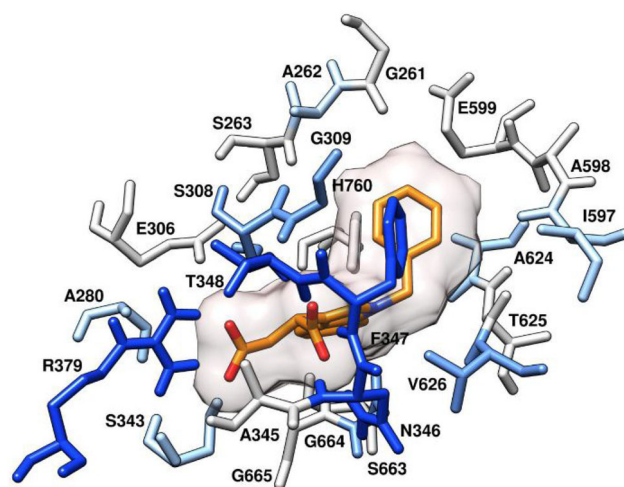
In order to further confirm the ACLY inhibition activity of compound VS1, both this compound and HCA were subjected to an enzymatic inhibition test using the ADP-Glo assay (Jernigan et al., 2017). Interestingly, the biological data highlighted an inhibitory activity at a concentration of 400 μM ranging from 52% for VS1 to 31% for HCA, thus confirming the higher inhibition activity of VS1 with respect to HCA. As shown in Figure 4, the two carboxylic groups of VS1 properly mimic the interactions observed for citrate in its X-ray complex with ACLY. In fact, the carboxylic group closer to the indole core of the ligand forms the three essential H-bonds with the backbone nitrogen of N346, F347 and T348, showing also the additional H-bonds with the side chain of N346 and the hydroxyl group of T348, which were maintained for almost the whole MD simulation. The other carboxylic group forms a stable salt bridge with R379 and an additional H-bond with the hydroxyl group of S343, not observed in the ACLY-citrate X-ray structure, which is, however, formed only for about 50% of the MD. The indole core

Table 4. Biological assay result.

#	S ID	Structure	IC ₅₀ (μM)
VS1	30038443		191 ± 15
VS2	124834010		> 500
VS3	28145009		> 500
VS4	53231107		> 500
VS5	27121891		> 500
VS6	321780087		> 500
HCA			465 ± 21

of the ligand lays on S663, G664 and G665, also interacting with S308 and H760. Finally, the *N*-benzyl group of the compound is placed in a predominantly hydrophobic pocket mainly delimited by G309, F347, I597, A624, V626 and H760, thus forming lipophilic interactions with all these residues and, in particular, a π - π stacking with, F347.

In addition, we analyzed the predicted binding mode of VS1 from the energetic point of view. VS1 was subjected to ligand-protein binding energy evaluations performed using the Molecular Mechanics-Generalized Born Surface Area (MM-GBSA) method. The whole 20 ns of MD simulations were employed to estimate the binding free energy associated with VS1 from its corresponding ligand-protein complex and a binding energy of -102.1 kcal/mol was estimated. Then, an in-depth analysis of the ligand-protein binding interactions was carried out with the aim of identifying and validating the key residues, among those predicted to interact with the ligand by the docking-MD protocol, which may have a pivotal role for the inhibitory activity of VS1. MM-GBSA approach with pairwise per-residue energy decomposition was employed to calculate the contribute to the ligand binding affinity of each single amino acid surrounding VS1 in the catalytic site of ACLY. The analysis highlighted four fundamental amino acid residues that provided a major contribute to the total

**Figure 4.** Minimized average structure of VS1-ACLY complex.**Figure 5.** Minimized average structure of VS1 on ACLY. The residues are colored based on their contribution to ligand-protein binding energy (blue = highest, white = lowest).

ligand-protein binding energy and corresponded to the key anchoring residues taken into account in the pharmacophore model and post-docking filter employed in our VS workflow: R379, T348, F347 and N346 (Figure 5). Unsurprisingly, R379, forming a stable salt bridge interaction with VS1 that was maintained for the whole MD simulation, was confirmed to be the residue with the highest impact on the binding free energy, showing an individual energetic contribute of -32.3 kcal/mol. Another very high contribute to the binding free energy, corresponding to -24.0 kcal/mol, was calculated for N346; although such a high value might not be expected for this residue, it is consistent with the MD results showing a high stability of both the H-bonds between VS1, the backbone nitrogen and the side chain of N346. Finally, a similarly high energetic contribute of -11.8 and -10.4 kcal/mol was calculated for T348 and F347, respectively. In fact, while T348 formed two different H-bonds with the ligand, F347 showed a single H-bond but also a T-shaped π - π stacking with the benzyl ring of VS1, which undoubtedly improved the binding affinity of the ligand. Together, the four key residues R379, T348, F347 and N346 were estimated to determine a total of -78.5 kcal/mol out of the overall ligand-protein binding energy of -102.1 kcal/mol. On the contrary, S343, forming only a

transient H-bond with VS1, showed a much lower energy contribution of -2.5 kcal/mol. Therefore, the per-residue MM-GBSA analysis confirmed the importance of the predicted ligand-protein interactions and the fundamental H-bonds showed also by citrate that were taken into account in our VS study. Moreover, this analysis highlighted a not negligible contribute to the binding energy for some of the residues constituting the hydrophobic cleft near the substrate binding domain and especially for those placed in proximity of F347, such as, V626 (Figure 5), which showed an energetic contribute of -4.0 kcal/mol. This could suggest a possible hit optimization strategy based on the exploration of the hydrophobic cleft for the design of new VS1 analogues that may better fill this cavity by forming stronger interactions with the residues at the entrance of ACLY binding site.

Conclusion

We have developed a pharmacophore-based VS study to identify new ACLY inhibitors against cancer. A receptor-based pharmacophore screening supported by hierarchical docking, consensus docking and molecular dynamics simulations, further refined by binding free energy calculations of ligand-protein complexes, led us to the identification of compound VS1 as a promising hit compound. Although VS1 was not found to be a particularly potent ACLY inhibitor, showing an IC_{50} of 191 μ M, it however proved to be 2.5-fold stronger than the well-known ACLY inhibitor 2-HCA, which was used as a reference in our enzyme assays. These results confirmed the reliability of our VS protocol. The binding mode predicted for VS1 showed that the ligand can properly reproduce the interactions of the endogenous ligand with the key anchoring residues of the enzyme, whose crucial contribution to the ligand-protein binding affinity was also investigated through binding free energy evaluations. This analysis highlighted the hydrophobic cleft of ACLY, adjacent to the substrate binding domain, as a potential site to be targeted in further hit optimization studies focused on the development of more potent inhibitors by better occupying the wide excluded volume of the cleft. We believe that the outcome of our study gives medicinal chemists a significant tool for the rational design of highly potent ACLY inhibitors to be used as potential anticancer agents.

Materials and methods

Pharmacophore model generation

The pharmacophore model was constructed using LigandScout 4.2. The pharmacophore hypothesis was generated from the X-ray structure of human ACLY in complex with citrate (PDB ID: 5TDE). A complete model including all the possible pharmacophore features recognized by the program was initially generated and all the features were taken into consideration in the final pharmacophore model, for a total of 7 H-bond acceptor features. Four pharmacophore features were set as mandatory and the three other features were set as optional. The excluded volume spheres, defined

by the default LigandScout configuration, illustrating the regions of space in the proximity of the pharmacophore model occupied by the enzyme, were also taken into consideration within the pharmacophore model.

Database generation and pharmacophore screening

Around 2.5 million compounds in total, obtained from Enamine and Vitas-M commercial databases, were used as the screening database. The software iCon (Poli et al., 2018) implemented in LigandScout was used to perform ligand conformational sampling and to set up the 3D database. The generated pharmacophore model including the four mandatory features, the three optional features and the excluded volume spheres was used to screen the 3D database and to search for desirable compounds. Only compounds matching at least the four mandatory features of the model and respecting the excluded volume constraints were retrieved in this search.

Molecular docking and pose filtering

All docking calculations were carried out using the X-ray structure of human ACLY in complex with citrate (PDB ID: 5TDE) already employed for pharmacophore modeling. Twelve different docking procedures were used in this study: AutoDock 4.2.3, Autodock Vina 1.1, Dock 6.7, Fred 3.0, GlamDock, Gold 5.1 with its four fitness functions (i.e. ChemScore, GoldScore, ChemPLP and Astex Statistical Potential), Glide 5.0 with standard precision (SP) and extra precision (XP) methods and Plants, according to the procedures described in our previous studies (Pini et al., 2018; Tuccinardi et al., 2014). Self-docking analysis for each docking program was performed by calculating the root-mean-square deviation (RMSD) between the position of the endogenous ligand predicted by docking and its known experimental disposition, using the rms_analysis software of Gold suite. The filtering of the docking results was performed by superimposing the docked compounds to the pharmacophore model directly from the supplied poses, without changing their coordinates. The retrieval of compounds matching the four mandatory features of the model was imposed in this search.

Consensus docking evaluation

The consensus docking evaluation was performed on the ligands survived to the last docking step and thus docked into ACLY binding site using 11 different docking methods. A total of 11 different binding dispositions (top-ranked docking poses) were thus obtained for each compound. The RMSD of each docking pose versus the remaining others was calculated by means of the rms_analysis software of the Gold suite and an 11×11 matrix reporting the RMSD results was generated. With the application of an in-house program, results were clustered so that similar docking poses were grouped together. The complete-linkage method was employed as hierarchical clustering algorithm, with an RMSD

threshold of 2.0 Å. As a result, the clusters obtained included only those poses that were less than 2.0 Å away from one another. The consensus level of each ligand was defined as the number of docking poses that were clustered together within the 2.0 Å RMSD cut-off and thus as the number of docking methods generating similar binding poses.

MD Simulations

All simulations were carried out using AMBER 16. General amber force field (GAFF) parameters were assigned to the ligands, while partial charges were determined using the AM1-BCC method as implemented in the Antechamber suite (AMBER16). Ligand-protein complexes were placed in a rectangular parallelepiped water-box, by using TIP3P explicit solvent model, and solvated with a 20.0 Å water cap. Chlorine ions were added as counterions in order to neutralize the systems. Before MD simulations, two stages of minimization were carried out; in the first step, a position restraint of 100 kcal/(mol·Å²) was applied to the complex, thus minimizing only the position of the water molecules through 5000 steps of steepest descent followed by conjugate gradient, until a convergence of 0.05 kcal/(mol·Å²). Successively, the whole system was energy minimized imposing a harmonic force constant of 10 kcal/(mol·Å²) only to the protein α carbons. Periodic boundary conditions and Particle mesh Ewald (PME) electrostatics were employed in the simulations. The minimized complexes were used as starting conformations for the MD simulations. The time step of the simulations was 2 fs, a cut-off of 10.0 Å was set for the non-bonded interactions and SHAKE algorithm was used to keep all bonds involving hydrogen atoms rigid. Constant-volume MD simulation was performed for the first 0.5 ns, during which the temperature of the system was raised from 0 to 300 K. Then 19.5 ns of constant-pressure periodic boundary MD was carried out at 300 K, employing the Langevin thermostat in order to keep constant the temperature of the system. Thus, a 20 ns MD simulation was performed for each ligand-protein complex analyzed in this study. In detail, a position restraint of 10 kcal/(mol·Å²) was applied to the protein α carbons during the first 3.5 ns, while in remaining 16.5 ns no constraint was applied and the system was maintained completely free. All the obtained MD trajectories were analyzed using the Cpptraj program implemented in AMBER 16.

Binding energy evaluation

The ligand-protein binding affinity of the ACLY-VS1 complex and the pairwise per-residue free energy decomposition were calculated with AMBER 16 using the MM-GBSA method. The trajectories corresponding to whole 20 ns of MD simulation were used for the evaluation, which was performed on a total of 200 MD frames (one every 100 ps). MOLSURF program and the MM-PBSA module of AMBER 16 were used to calculate nonpolar and polar energies, respectively, while SANDER module estimated van der Waals, electrostatic, and

internal contributions. The ligand's entropy was not taken into account in the calculation (Granchi et al., 2019).

Enzymatic assays

Enzymatic assays were performed by using recombinant human ACLY (Merck-Sigma Aldrich) and the malate dehydrogenase coupled-enzyme assay was adopted, conducted as described previously (Gribble et al., 1996).

The assay was performed in 96-well plates. The ACLY reaction was carried out at room temperature, at a final volume of 50 μ L in the assay buffer of 40 mM Tris, pH 8.0, 10 mM MgCl₂, 5 mM DTT. The final concentration of DMSO was 1% (v/v). The final concentrations of the substrates were 100 μ M ATP, 200 μ M CoA, and 200 μ M sodium citrate. The reaction was initiated by the addition of 10 μ L of ACLY (20 ng/well); after the reaction had proceeded for 30 min, the ACLY activity was determined by the malate dehydrogenase-catalyzed reduction of oxaloacetate by NADH (20 μ L of a solution of MDH and 80 μ M NADH). NADH consumption was measured by monitoring the reaction at 340 nm. Two reactions were also run: one reaction containing no compounds and the second one containing neither compound nor ACLY. To remove possible false positive results, for each compound concentration a blank analysis was carried out, and the final absorbance results were obtained subtracting the absorbance produced by the presence of all the components except ACLY in the same conditions.

The enzyme inhibition activity was also confirmed using the ADP-Glo kit (Promega), as described previously (Jernigan et al., 2017). Compounds VS1 and HCA at a final concentration of 400 μ M were added to 12.5 μ L of recombinant human ACLY (30 ng) in the assay buffer of 40 mM Tris, pH 8.0, 10 mM MgCl₂, 5 mM DTT. The reaction was started by adding 100 μ M ATP, 200 μ M CoA, and 200 μ M sodium citrate. The total volume of reaction is 25 μ L and the final concentration of DMSO was 1% in all reactions. The enzymatic reactions were performed at room temperature for 60 min. After the reaction, the amount of ADP was quantified using ADP-Glo luminescence assay kit according to the manufacturer's instruction.

Disclosure statement

No potential conflict of interest was reported by the author(s).

ORCID

Lidia Ciccone  <http://orcid.org/0000-0002-2762-1929>
 Filippo Minutolo  <http://orcid.org/0000-0002-3312-104X>
 Flavio Rizzolio  <http://orcid.org/0000-0002-3400-4363>
 Carlotta Granchi  <http://orcid.org/0000-0002-5849-0722>
 Tiziano Tuccinardi  <http://orcid.org/0000-0002-6205-4069>

References

Amaravathi, H., Baek, K., & Yoon, H. (2014). Revisiting *de novo* drug design: Receptor based pharmacophore screening. *Current Topics in*

- Medicinal Chemistry*, 14(16), 1890–1898. <https://doi.org/10.2174/1568026614666140929115506>
- Beckner, M. E., Fellows-Mayle, W., Zhang, Z., Agostino, N. R., Kant, J. A., Day, B. W., & Pollack, I. F. (2010). Identification of ATP citrate lyase as a positive regulator of glycolytic function in glioblastomas. *International Journal of Cancer*, 126(10), NA–2295. <https://doi.org/10.1002/ijc.24918>
- Bertilsson, H., Tessem, M.-B., Flatberg, A., Viset, T., Gribbestad, I., Angelsen, A., & Halgunset, J. (2012). Changes in gene transcription underlying the aberrant citrate and choline metabolism in human prostate cancer samples. *Clinical Cancer Research*, 18(12), 3261–3269. <https://doi.org/10.1158/1078-0432.CCR-11-2929>
- Breen, M. E., & Soellner, M. B. (2015). Small molecule substrate phosphorylation site inhibitors of protein kinases: Approaches and challenges. *ACS Chemical Biology*, 10(1), 175–189. <https://doi.org/10.1021/cb5008376>
- Deng, Z., Wong, N.-K., Guo, Z., Zou, K., Xiao, Y., & Zhou, Y. (2019). Dehydrocurvularin is a potent antineoplastic agent irreversibly blocking ATP-citrate lyase: Evidence from chemoproteomics. *Chemical Communications (Cambridge, England)*, 55(29), 4194–4197. <https://doi.org/10.1039/c9cc00256a>
- Granchi, C. (2018). ATP citrate lyase (ACLY) inhibitors: An anti-cancer strategy at the crossroads of glucose and lipid metabolism. *European Journal of Medicinal Chemistry*, 157, 1276–1291. <https://doi.org/10.1016/j.ejmech.2018.09.001>
- Granchi, C. (2019). Discovery of allosteric inhibition of human ATP-citrate lyase. *Trends in Pharmacological Sciences*, 40(6), 364–366. <https://doi.org/10.1016/j.tips.2019.04.008>
- Granchi, C., Lapillo, M., Glasmacher, S., Bononi, G., Licari, C., Poli, G., El Boustani, M., Caligiuri, I., Rizzolio, F., Gertsch, J., Macchia, M., Minutolo, F., Tuccinardi, T., & Chicca, A. (2019). Optimization of a benzoylpiperidine class identifies a highly potent and selective reversible monoacylglycerol lipase (MAGL) inhibitor. *Journal of Medicinal Chemistry*, 62(4), 1932–1958. <https://doi.org/10.1021/acs.jmedchem.8b01483>
- Gribble, A. D., Dolle, R. E., Shaw, A., McNair, D., Novelli, R., Novelli, C. E., Slingsby, B. P., Shah, V. P., Tew, D., Saxty, B. A., Allen, M., Groot, P. H., Pearce, N., & Yates, J. (1996). ATP-Citrate Lyase as a target for hypolipidemic intervention. Design and synthesis of 2-substituted butanedioic acids as novel, potent inhibitors of the enzyme. *Journal of Medicinal Chemistry*, 39(18), 3569–3584. <https://doi.org/10.1021/jm960167w>
- Hatzivassiliou, G., Zhao, F., Bauer, D. E., Andreadis, C., Shaw, A. N., Dhanak, D., Hingorani, S. R., Tuveson, D. A., & Thompson, C. B. (2005). ATP citrate lyase inhibition can suppress tumor cell growth. *Cancer Cell*, 8(4), 311–321. <https://doi.org/10.1016/j.ccr.2005.09.008>
- Hoffmann, G. E., Andres, H., Weiss, L., Kreisel, C., & Sander, R. (1980). Lipogenesis in man: Properties and organ distribution of ATP citrate (pro-3S)-lyase. *Biochimica et Biophysica Acta (BBA) - Lipids and Lipid Metabolism*, 620(1), 151–158. [https://doi.org/10.1016/0005-2760\(80\)90194-0](https://doi.org/10.1016/0005-2760(80)90194-0)
- Hu, J., Komakula, A., & Fraser, M. E. (2017). Binding of hydroxycitrate to human ATP-citrate lyase. *Acta Crystallographica. Section D, Structural Biology*, 73(Pt 8), 660–671. <https://doi.org/10.1107/S2059798317009871>
- Jernigan, F. E., Hanai, J., Sukhatme, V. P., & Sun, L. (2017). Discovery of furan carboxylate derivatives as novel inhibitors of ATP-citrate lyase via virtual high-throughput screening. *Bioorganic & Medicinal Chemistry Letters*, 27(4), 929–935. <https://doi.org/10.1016/j.bmcl.2017.01.001>
- Ki, S. W., Ishigami, K., Kitahara, T., Kasahara, K., Yoshida, M., & Horinouchi, S. (2000). Radicol binds and inhibits mammalian ATP citrate lyase. *The Journal of Biological Chemistry*, 275(50), 39231–39236. <https://doi.org/10.1074/jbc.M006192200>
- Kuo, C.-Y., & Ann, D. K. (2018). When fats commit crimes: Fatty acid metabolism, cancer stemness and therapeutic resistance. *Cancer Communications (London, England)*, 38(1), 47. <https://doi.org/10.1186/s40880-018-0317-9>
- Lapillo, M., Salis, B., Palazzolo, S., Poli, G., Granchi, C., Minutolo, F., Rotondo, R., Caligiuri, I., Canzonieri, V., Tuccinardi, T., & Rizzolio, F. (2019). First-of-its-kind STARD3 inhibitor: In silico identification and biological evaluation as anticancer agent. *ACS Medicinal Chemistry Letters*, 10(4), 475–480. <https://doi.org/10.1021/acsmedchemlett.8b00509>
- Li, J. J., Wang, H., Tino, J. A., Robl, J. A., Herpin, T. F., Lawrence, R. M., Biller, S., Jamil, H., Ponticello, R., Chen, L., Chu, C.-h., Flynn, N., Cheng, D., Zhao, R., Chen, B., Schnur, D., Obermeier, M. T., Sasseville, V., Padmanabha, R., Pike, K., & Harrity, T. (2007). 2-Hydroxy-N-arylbenzenesulfonamides as ATP-citrate lyase inhibitors. *Bioorganic & Medicinal Chemistry Letters*, 17(11), 3208–3211. <https://doi.org/10.1016/j.bmcl.2007.03.017>
- Menendez, J. A., & Lupu, R. (2007). Fatty acid synthase and the lipogenic phenotype in cancer pathogenesis. *Nature Reviews. Cancer*, 7(10), 763–777. <https://doi.org/10.1038/nrc2222>
- Migita, T., Narita, T., Nomura, K., Miyagi, E., Inazuka, F., Matsuura, M., Ushijima, M., Mashima, T., Seimiya, H., Satoh, Y., Okumura, S., Nakagawa, K., & Ishikawa, Y. (2008). ATP citrate lyase: Activation and therapeutic implications in non-small cell lung cancer. *Cancer Research*, 68(20), 8547–8554. <https://doi.org/10.1158/0008-5472.CAN-08-1235>
- Pearce, N. J., Yates, J. W., Berkhout, T. A., Jackson, B., Tew, D., Boyd, H., Camilleri, P., Sweeney, P., Gribble, A. D., Shaw, A., & Groot, P. H. E. (1998). The role of ATP citrate-lyase in the metabolic regulation of plasma lipids Hypolipidaemic effects of SB-204990, a lactone prodrug of the potent ATP citrate-lyase inhibitor SB-201076. *Biochemical Journal*, 334(1), 113–119. <https://doi.org/10.1042/bj3340113>
- Pini, E., Poli, G., Tuccinardi, T., Chiarelli, L., Mori, M., Gelain, A., Costantino, L., Villa, S., Meneghetti, F., & Barlocco, D. (2018). New chromane-based derivatives as inhibitors of mycobacterium tuberculosis salicylate synthase (MbtI): Preliminary biological evaluation and molecular modeling studies. *Molecules*, 23(7), 1506. <https://doi.org/10.3390/molecules23071506>
- Poli, G., Martinelli, A., & Tuccinardi, T. (2016). Reliability analysis and optimization of the consensus docking approach for the development of virtual screening studies. *Journal of Enzyme Inhibition and Medicinal Chemistry*, 31(sup2), 167–173. <https://doi.org/10.1080/14756366.2016.1193736>
- Poli, G., Seidel, T., & Langer, T. (2018). Conformational sampling of small molecules with iCon: Performance assessment in comparison with OMEGA. *Frontiers in Chemistry*, 6, 229. <https://doi.org/10.3389/fchem.2018.00229>
- Russo Spena, C., De Stefano, L., Poli, G., Granchi, C., El Boustani, M., Ecça, F., Grassi, G., Grassi, M., Canzonieri, V., Giordano, A., Tuccinardi, T., Caligiuri, I., & Rizzolio, F. (2019). Virtual screening identifies a PIN1 inhibitor with possible antiovarian cancer effects. *Journal of Cellular Physiology*, 234(9), 15708–15716. <https://doi.org/10.1002/jcp.28224>
- Suburu, J., & Chen, Y. Q. (2012). Lipids and prostate cancer. *Prostaglandins & Other Lipid Mediators*, 98(1–2), 1–10. <https://doi.org/10.1016/j.prostaglandins.2012.03.003>
- Sun, T., Hayakawa, K., & Fraser, M. E. (2011). ADP-Mg2+ bound to the ATP-grasp domain of ATP-citrate lyase. *Acta Crystallographica. Section F, Structural Biology and Crystallization Communications*, 67(Pt 10), 1168–1167. <https://doi.org/10.1107/S1744309111028363>
- Swinnen, J. V., Brusselmans, K., & Verhoeven, G. (2006). Increased lipogenesis in cancer cells: New players, novel targets. *Current Opinion in Clinical Nutrition and Metabolic Care*, 9(4), 358–365. <https://doi.org/10.1097/01.mco.0000232894.28674.30>
- Tuccinardi, T. (2009). Docking-based virtual screening: Recent developments. *Combinatorial Chemistry & High Throughput Screening*, 12(3), 303–314. <https://doi.org/10.2174/138620709787581666>
- Tuccinardi, T., Poli, G., Corchia, I., Granchi, C., Lapillo, M., Macchia, M., Minutolo, F., Ortore, G., & Martinelli, A. (2016). A virtual screening study for lactate dehydrogenase 5 inhibitors by using a pharmacophore-based approach. *Molecular Informatics*, 35(8–9), 434–439. <https://doi.org/10.1002/minf.201501026>
- Tuccinardi, T., Poli, G., Romboli, V., Giordano, A., & Martinelli, A. (2014). Extensive consensus docking evaluation for ligand pose prediction and virtual screening studies. *Journal of Chemical Information and Modeling*, 54(10), 2980–2986. <https://doi.org/10.1021/ci500424n>
- Verschueren, K. H. G., Blanchet, C., Felix, J., Dansercoer, A., De Vos, D., Bloch, Y., Van Beeumen, J., Svergun, D., Gutsche, I., Savvides, S. N., &

- Verstraete, K. (2019). Structure of ATP citrate lyase and the origin of citrate synthase in the Krebs cycle. *Nature*, 568(7753), 571–575. <https://doi.org/10.1038/s41586-019-1095-5>
- Wang, Y., Wang, Y., Shen, L., Pang, Y., Qiao, Z., & Liu, P. (2012). Prognostic and therapeutic implications of increased ATP citrate lyase expression in human epithelial ovarian cancer. *Oncology Reports*, 27(4), 1156–1162. <https://doi.org/10.3892/or.2012.1638>
- Wang, J., Ye, W., Yan, X., Guo, Q., Ma, Q., Lin, F., Huang, J., & Jin, J. (2019). Low expression of ACLY associates with favorable prognosis in acute myeloid leukemia. *Journal of Translational Medicine*, 17(1), 149. <https://doi.org/10.1186/s12967-019-1884-5>
- Wei, J., Leit, S., Kuai, J., Therrien, E., Rafi, S., Harwood, H. J., DeLaBarre, B., & Tong, L. (2019). An allosteric mechanism for potent inhibition of human ATP-citrate lyase. *Nature*, 568(7753), 566–570. <https://doi.org/10.1038/s41586-019-1094-6>
- Wolber, G., & Langer, T. (2005). LigandScout: 3-D pharmacophores derived from protein-bound ligands and their use as virtual screening filters. *Journal of Chemical Information and Modeling*, 45(1), 160–169. <https://doi.org/10.1021/ci049885e>
- Yahagi, N., Shimano, H., Hasegawa, K., Ohashi, K., Matsuzaka, T., Najima, Y., Sekiya, M., Tomita, S., Okazaki, H., Tamura, Y., Iizuka, Y., Ohashi, K., Nagai, R., Ishibashi, S., Kadowaki, T., Makuuchi, M., Ohnishi, S., Osuga, J.-i., & Yamada, N. (2005). Co-ordinate activation of lipogenic enzymes in hepatocellular carcinoma. *European Journal of Cancer (Oxford, England : 1990)*, 41(9), 1316–1322. <https://doi.org/10.1016/j.ejca.2004.12.037>
- Zadra, G., Photopoulos, C., & Loda, M. (2013). The fat side of prostate cancer. *Biochimica et Biophysica Acta*, 1831(10), 1518–1532. <https://doi.org/10.1016/j.bbailip.2013.03.010>
- Zaidi, N., Swinnen, J. V., & Smans, K. (2012). ATP-citrate lyase: A key player in cancer metabolism. *Cancer Research*, 72(15), 3709–3714. <https://doi.org/10.1158/0008-5472.CAN-11-4112>
- Zhao, S., Torres, A., Henry, R. A., Trefely, S., Wallace, M., Lee, J. V., Carrer, A., Sengupta, A., Campbell, S. L., Kuo, Y.-M., Frey, A. J., Meurs, N., Viola, J. M., Blair, I. A., Weljie, A. M., Metallo, C. M., Snyder, N. W., Andrews, A. J., & Wellen, K. E. (2016). ATP-citrate lyase controls a glucose-to-acetate metabolic switch. *Cell Reports*, 17(4), 1037–1052. <https://doi.org/10.1016/j.celrep.2016.09.069>